ROYAL SOCIETY
OF CHEMISTRY

PAPER

Check for updates

A non-toxic triboelectric nanogenerator for baby care applications†

Kang Yan,‡[a] Xiao Li,‡[a] Xiao-Xiong Wang,*[af] Miao Yu,[c] Zhiyong Fan, [ID][b]
Seeram Ramakrishna, [ID][d] Han Hu [ID][e] and Yun-Ze Long [ID]*[a]

Children often face more dangers than adults because of their unsound awareness of self-protection. Ensuring that modern technology is child safe has become an important research field. Conventional household electricity is dangerous for babies due to its high voltage. Considering that babies like to bite, some common low-voltage energy sources, such as lithium-ion batteries, also present certain risks. Therefore, the development of non-toxic and harmless energy sources for children is urgently needed. Considering that children tend to be more active than adults, nanogenerators are ideal for such applications, due to their effective use of abundant mechanical energy, and they will not cause the risk of electric shock or poisoning by accidental swallowing. Herein, we report a triboelectric nanogenerator (TENG) based on carboxymethyl chitosan (CMCS) and carboxymethyl cellulose sodium (CMC-Na). The TENG can dissolve quickly when it encounters water, and it will not affect the environment after dissolution. We measured the electrical performance of the TENG with an effective area of 3×3 cm^2 under a frequency of 2 Hz. The output power of this TENG can reach 120 mW m^{-2}. Meanwhile, it contains no flavor, which avoids active consumption by children. It can continuously power electronic watches, temperature-hygrometers, and calculators. In addition, we confirmed the edibility of the TENG through feeding experiments. Even if a baby eats it by mistake, it will not affect the baby's health. The good infrared transmission effect allows this material to be used in baby diapers and other applications to dissipate heat and improve wearing comfort.

1. Introduction

Nanogenerators (NGs) use displacement current as the driving force for effectively converting mechanical energy into electric power. Different types of NG, including triboelectric nanogenerators (TENGs), piezoelectric nanogenerators (PENGs) and pyroelectric nanogenerators, use different methods of energy generation. NGs have been widely used in energy,[1–8] medical monitoring[9,10] and other applications.[11–16] As a typical NG, TENGs have high efficiency output. In one in-depth study of

a TENG, its output voltage was increased to hundreds of volts.[17] At the same time, TENGs have also proven to be simple, low-cost, robust and environmentally friendly.[18,19]

TENGs use the electronegativity of materials to generate electricity. Charge transfer occurs when two materials of different electronegativities contact. Therefore, TENGs can collect various types of mechanical energy. In addition, displacement of self-powered sensors,[20–23] speed,[24–26] metal ions,[27] humidity,[28] temperature[29] and other physical parameters can also be detected by TENGs by converting various forms of energy into electrical signals. Nanofibers prepared by electrospinning have the characteristics of large specific surface area and high porosity, and have been widely used in drug delivery,[30] wound dressings,[31] air filtration,[32,33] energy collection[34] and so on.[35–38] Carboxymethyl chitosan (CMCS) is a water-soluble chitosan derivative with many features such as potent antimicrobial activity, freshness retention effect, and amphoteric polyelectrolyte properties. This material has various uses in cosmetics, fresh key pressing[39] and medicine.[40] Carboxymethyl cellulose sodium (CMC-Na) is used as a thickener in the food industry and as a pharmaceutical carrier in medicine.[41]

Traditional TENGs use molten polymer materials or toxic solvents in the preparation process, and other materials that can affect people's health, such as carbon nanotubes.[42]

[a]*Collaborative Innovation Center for Nanomaterials & Devices, College of Physics, Qingdao University, Qingdao 266071, China. E-mail: yunze.long@qdu.edu.cn; wangxiaoxiong69@163.com; Tel: +86 139 5329 0681*

[b]*Department of Electronic & Computer Engineering, The Hong Kong University of Science & Technology, Kowloon, Hong Kong, China*

[c]*Department of Mechanical Engineering, Columbia University, New York, NY 10027, USA*

[d]*Center for Nanofibers & Nanotechnology, National University of Singapore, Singapore*

[e]*State Key Laboratory of Heavy Oil Processing, College of Chemical Engineering, China University of Petroleum (East China), Qingdao, 266580, China*

[f]*State Key Laboratory of Bio-Fibers and Eco-Textiles, Qingdao University, Qingdao 266071, China*

† Electronic supplementary information (ESI) available. See DOI: 10.1039/d0ta08909e

‡ These two authors contributed equally to this work.

Therefore, TENGs can easily cause harm to the environment and the human body, meaning that they should certainly not be used in baby products. In this work, we used environmentally friendly preparation methods to avoid the negative impact of TENGs on the environment. We designed a TENG prepared using CMCS and CMC-Na. It uses a dual-motor structure and has a high output power.[43] It can dissolve quickly in water, and there are no side effects, even if swallowed.

2.   Experimental section

2.1.   Materials

CMCS (M_w: 80 000–250 000) was purchased from Cool Chemistry. CMC-Na (viscosity: 300–800 mPa s) was purchased from Aladdin Industrial Corporation. Polyethylene oxide (PEO, M_w: 5 000 000) was purchased from Macklin. Edible gold leaf was purchased online.

2.2.   Preparation of solutions

The CMCS powder and PEO powder (10/1 w/w) were dissolved in deionized water and then stirred with a magnetic stirrer for 8 h to prepare a CMCS solution (7 wt%). The CMC-Na powder and PEO powder (6/1 w/w) were dissolved in deionized water and then stirred at 70 °C for 8 h with a magnetic stirrer to prepare a CMC-Na solution (3 wt%).

2.3.   Fabrication of the TENG

CMCS solution was injected into a 10 mL syringe; the feed rate of the precursor was adjusted to 0.4 mL h^{-1} with a syringe pump (LSP01-1A, Baoding Long Precision Pump Co., Ltd., LSP1-1A). Aluminum foil was wrapped around a roller of 10 cm in

diameter and 20 cm in length, which was used as a collector; the rotation speed was 500 rpm, the spinning distance was 17 cm, and the electrospinning voltage was 18 kV between the needle and the collector. After 3 h, a two-dimensional uniform electrospun CMCS nanofiber membrane was obtained. A CMC-Na nanofiber membrane could be obtained by using the same method and conditions. The CMCS nanofiber membrane and CMC-Na nanofiber membrane were fabricated at a temperature of 27 ± 3 °C and humidity of 35 ± 5%. The two nanofiber membranes with an area of 30 × 30 mm^2 were adhered to gold foil as a positive electrode material and a negative electrode material of the TENG. Fig. S2† shows a physics diagram of the TENG.

2.4.   Characterization and measurements of the TENG

Scanning electron microscopy (SEM, TM-1000, Hitachi) was used to analyze the surface morphology and microstructure of the fiber membrane. The output current signal of TENG was collected by a picoammeter (Keithley 6487), and the charging voltage of the capacitor was recorded by a digital multimeter (Rigol DM 3058). In order to supply periodic vibration, we used a homemade device, as shown in Fig. S1,† which could contact and separate periodically.[44] The CMCS and CMC-Na nanofiber membranes were examined using Fourier-transform infrared spectroscopy (FTIR, Thermo Scientific Nicolet iN10). In order to prove that the TENG is green and edible, we performed acute systemic toxicity tests of both the carboxymethyl chitosan nanofiber membrane and the carboxymethyl cellulose sodium nanofiber membrane. Tests were performed at Epin SuZhou Ltd (Building 4, No. 558 Fenhu Avenue, Wujiang District, SuZhou, China), and the experimental results proved
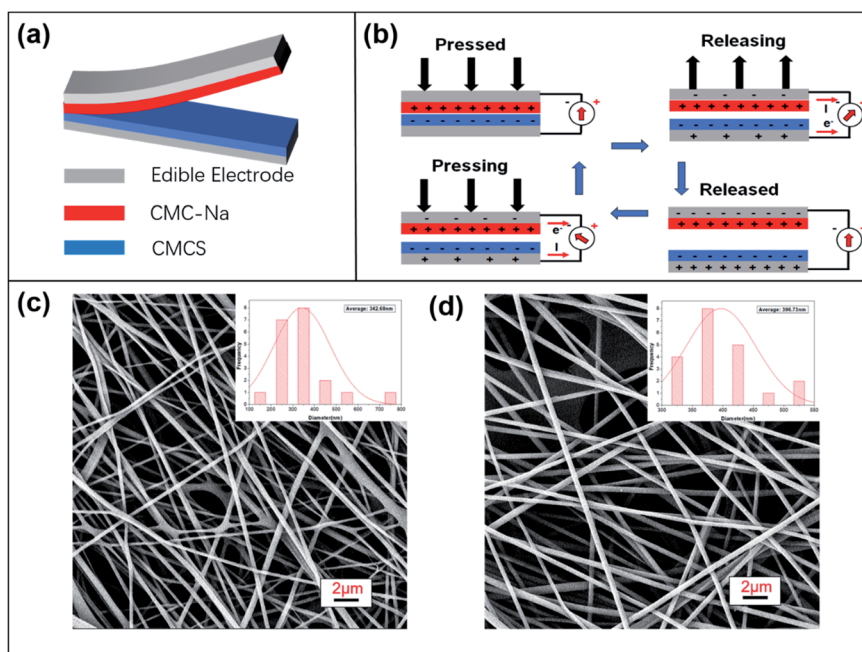
Fig. 1   (a) Schematic diagram of edible TENG. (b) A schematic diagram of the power generation principle of an edible TENG. (c) SEM images of CMCS and (d) CMC–Na nanofiber membranes.

that the mice who ate the CMCS nanofiber membrane and CMC-Na nanofiber membrane did not exhibit any abnormal clinical symptoms. The test process and results are shown in the ESI.†

3. Results and discussion

3.1. Basic characterization of the TENG

Fig. 1 shows a schematic diagram of the edible TENG. The basic structure is shown in Fig. 1a. It consists of a CMCS nanofiber membrane with a bottom electrode and a CMC-Na membrane with a top electrode. Fig. 1c and d show the surface morphology. The average diameters of the CMCS and CMC-Na nanofibers are 300 nm and 350 nm, respectively. Fig. 1b shows the working principle of the nanogenerator. The CMCS and CMC-Na nanofiber membranes serve as friction layers. In the initial state, the CMCS nanofiber membrane and the CMC-Na nanofiber membrane are in contact with each other without any current or potential. Due to the differences in surface electron affinity, electrons will be transferred from the surface of the CMC-Na nanofiber membrane to the CMCS nanofiber membrane. Therefore, the CMC-Na nanofiber membrane loses electrons and gains a positive charge, while the CMCS nanofiber membrane gets electrons and obtains a negative charge. When the two nanofiber membranes are separated, the charge separation creates a potential difference if they are connected to an external circuit, which generates a current. During the separation process, the open circuit voltage of the positive electrode gradually decreases until it drops to zero. When the two nanofiber membranes touch again, the current reverses.[45]

As shown in Fig. S3,† in order to test the flexibility of the nanofiber membrane, we folded the cut nanofiber membrane by 180°, and found that it could still return to its original state, indicating that the fiber film has good flexibility and can be used in fabrics. The nanofiber membrane will not be broken by bending and folding. In order to prove that the fiber membrane has good water solubility, we placed the CMCS fiber membrane and CMC-Na fiber membrane in deionized water, as shown in Fig. S4a.† The CMCS fiber nanofiber membrane was completely dissolved within 10 s. The pH of the solution was about 7. The dissolution process of CMC-Na is shown in Fig. S4b.† It had basically dissolved in 2 min and completely dissolved in 5 min. The pH of the solution was 6–7. Fig. S5† shows the tensile properties of CMCS and CMC-Na. It can be seen from the figure that the tensile ratio of the two nanofiber membranes is about 11%.

Fig. S6† shows the FTIR spectra of the nanofiber membranes. From Fig. S6a† we can get the chemical structure of CMCS. There are C–H tensile vibration peaks at 2939 cm^{-1} and 2883 cm^{-1}, N–H bending vibration peak at 1593 cm^{-1}, COO symmetrical vibration peak at 1411 cm^{-1}, CH_3 deformation vibration at 1316 cm^{-1}, and a C–O–C stretching vibration at 1100 cm^{-1}. Fig. S6b† shows the FTIR spectra of CMC-Na, with a C–H tensile vibration peak at 2940 cm^{-1}, N–H bending vibration peak at 1597 cm^{-1}, COO symmetrical vibration peak at 1416 cm^{-1}, C–H deformation vibration 1325 cm^{-1}, and C–O–C

stretching vibration peak at 1049 cm^{-1}. Therefore, the chemical properties of CMCS and CMC-Na before and after spinning are the same.

In order to prove that the nanogenerator is edible, we did an acute systemic toxicity test with ICR mice. The results are shown in Tables 1–4. Tables 1 and 2 show that the ICR mice of the test group and the negative control group both showed the same weight change. Tables 3 and 4 show that there are no signs of toxicity. Therefore, we proved that the nanogenerator is edible.

Table 1 Animal body weight results for CMCS

Group	No.	Weight (g)			
		0 h	24 h	48 h	72 h
Negative control	1101	18.69	19.52	20.42	21.28
	1102	19.95	20.21	21.10	22.00
	1103	20.12	21.22	22.09	23.13
	1104	21.25	22.15	23.00	24.02
	1105	21.91	22.71	23.56	24.38
Test group (CMCS)	2106	19.53	21.39	22.15	23.10
	2107	19.55	21.22	22.11	23.07
	2108	20.22	21.13	22.09	23.00
	2109	21.06	21.98	22.75	23.63
	2110	22.91	23.63	24.42	25.39

Table 2 Animal body weight results for CMC-Na

Group	No.	Weight (g)			
		0 h	24 h	48 h	72 h
Negative control	1101	18.95	19.86	20.73	21.69
	1102	19.95	20.89	21.77	22.86
	1103	21.06	21.94	22.55	23.48
	1104	21.25	22.36	23.18	24.00
	1105	21.91	22.63	23.52	24.60
Test group (CMC-Na)	2106	19.46	20.61	21.52	22.49
	2107	19.53	20.44	21.29	22.06
	2108	21.17	22.00	22.87	23.62
	2109	21.25	22.07	23.00	23.83
	2110	22.91	23.52	24.17	24.99

Table 3 Results of observed symptoms in mice after ingestion of CMCS

Group	No.	Symptoms				
		0 h	4 h	24 h	48 h	72 h
Negative control	1101	None	None	None	None	None
	1102	None	None	None	None	None
	1103	None	None	None	None	None
	1104	None	None	None	None	None
	1105	None	None	None	None	None
Test group (CMCS)	2106	None	None	None	None	None
	2107	None	None	None	None	None
	2108	None	None	None	None	None
	2109	None	None	None	None	None
	2110	None	None	None	None	None

Journal of Materials Chemistry A

Paper

Table 4 Results of observed symptoms in mice after ingestion of CMCS-Na

Group	No.	Symptoms				
		0 h	4 h	24 h	48 h	72 h
Negative control	1101	None	None	None	None	None
	1102	None	None	None	None	None
	1103	None	None	None	None	None
	1104	None	None	None	None	None
	1105	None	None	None	None	None
Test group (CMC-Na)	2106	None	None	None	None	None
	2107	None	None	None	None	None
	2108	None	None	None	None	None
	2109	None	None	None	None	None
	2110	None	None	None	None	None

3.2. Electrical performance of edible TENG

We assessed the output performance of the TENG through a series of electrical signal tests. As shown in Fig. 2a and b, the short-circuit current can reach 20 nA, and the open-circuit voltage can reach 3 V. In order to evaluate the electrical performance of the TENG in different environments, we tested its electrical performance under different humidity levels and different vibration frequencies, as shown in Fig. 2c and S7a.† We simulated environments with different levels of humidity: 60%, 50%, 40%, 30%, and 20% RH (relative humidity), with output currents of 2 nA, 2.5 nA, 5 nA, 8 nA, and 19 nA, respectively. This shows that the output of the TENG decreases as the ambient humidity increases. This is because humidity reduces the triboelectric effect and reduces the retention time of the triboelectric charge. Fig. 2d and S7b† show that as the impulse frequency increases, the short-circuit current increases proportionally. A higher pulse frequency can increase the magnitude of the short-circuit current because it shortens the duration of the current peak.

For practical applications, long-term stability and repeatability are crucial for TENGs. To test the long-term stability of the TENG, we performed 3000 cycles under the same conditions. As shown in Fig. 3a, the output current did not decrease, which shows that the TENG has excellent stability.

The relationship between electrical output and load resistance was also examined. As shown in Fig. 3b, the voltage gradually increased as the resistance increased and the current gradually decreased. We used the formula $P = \dfrac{U^2}{R}$ to obtain the power curve. As shown in Fig. 3c, the maximum load power density reached 120 mW m^{-2}, the external load resistance was 2 kΩ, and the corresponding current and voltage were 28 nA and 0.25 V, respectively, demonstrating better output performance than single-electrode form.[43] Capacitors can be used to store the pulsed energy of a TENG. As shown in Fig. 3d, a 47 μF
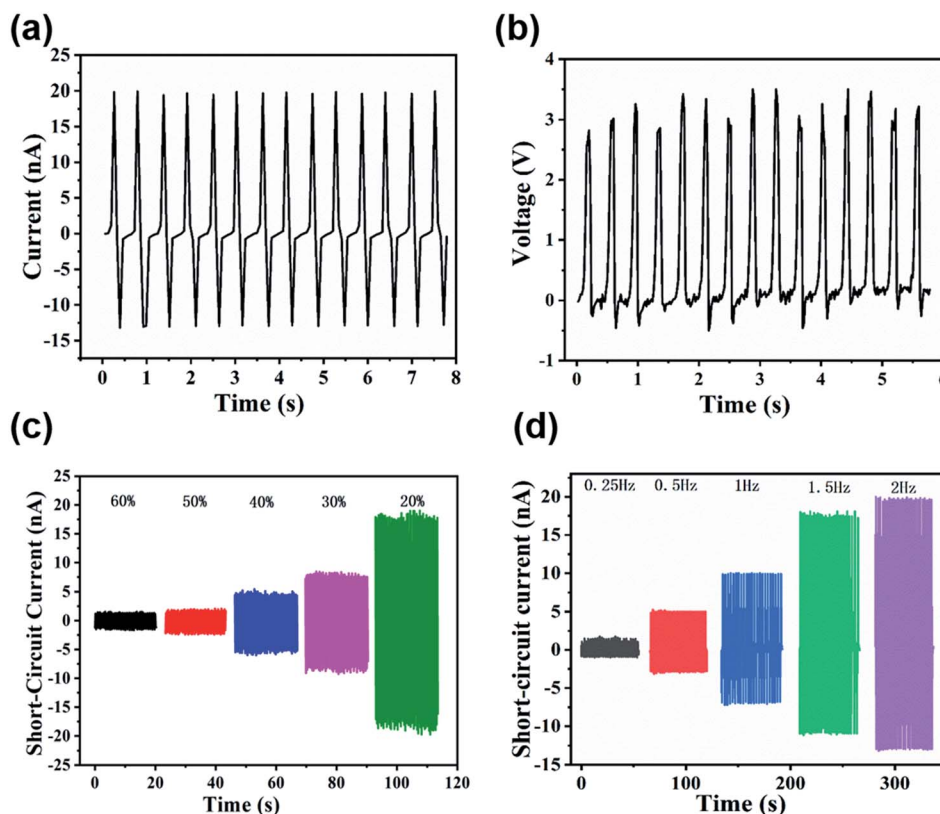
Fig. 2 Electrical performance of the TENG. (a) Short-circuit current and (b) open circuit voltage of the TENG under a frequency of 2 Hz. (c) Short-circuit current of the TENG at different atmospheric humidity levels and (d) impact frequency.
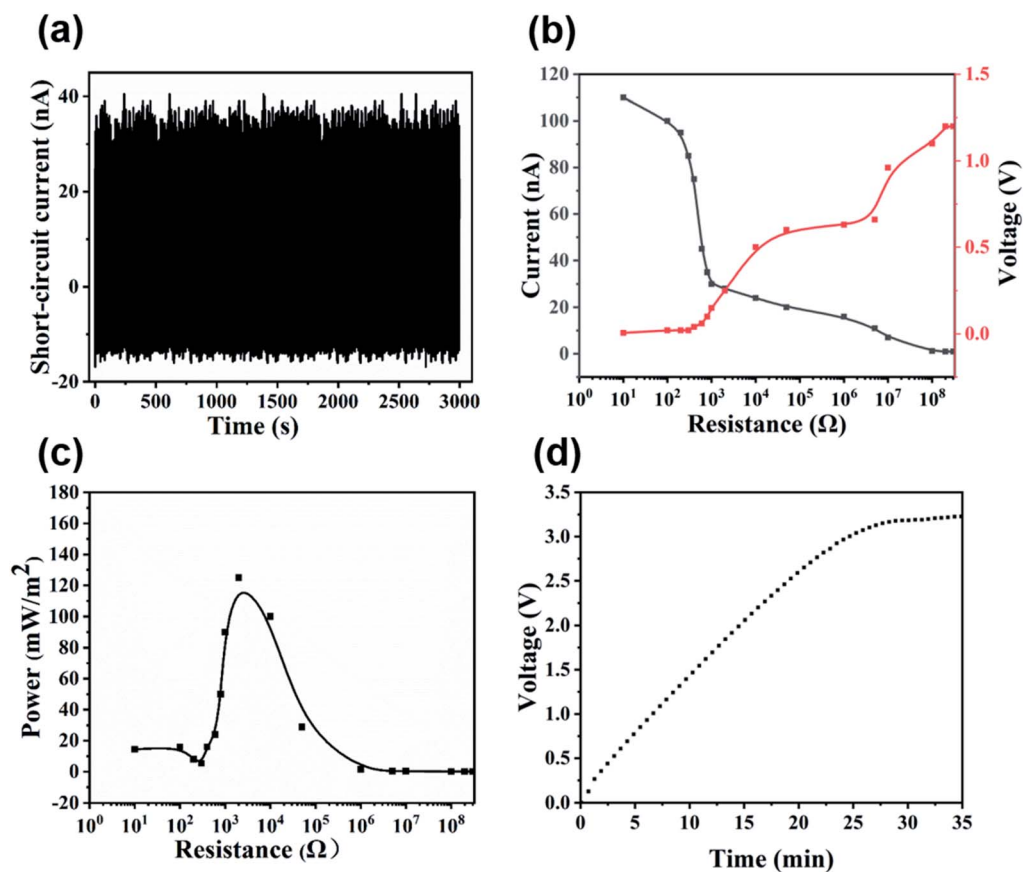
Fig. 3 Electrical performance of the TENG. (a) Electrical stability and durability test of the TENG. (b) Output current and voltage of the TENG with various external load resistances. (c) Dependence of output power on load resistance. (d) Charging curve of a 47 µF commercial capacitor by the TENG.

commercial capacitor can be charged using this TENG. This transforms the current to DC mode, which can power many microelectronic devices.

As the TENG is an energy harvesting device, it can be used in a variety of applications. We used a TENG with an area of 3×3 cm^2, as shown in Fig. 3d, and it could charge 47 µF commercial
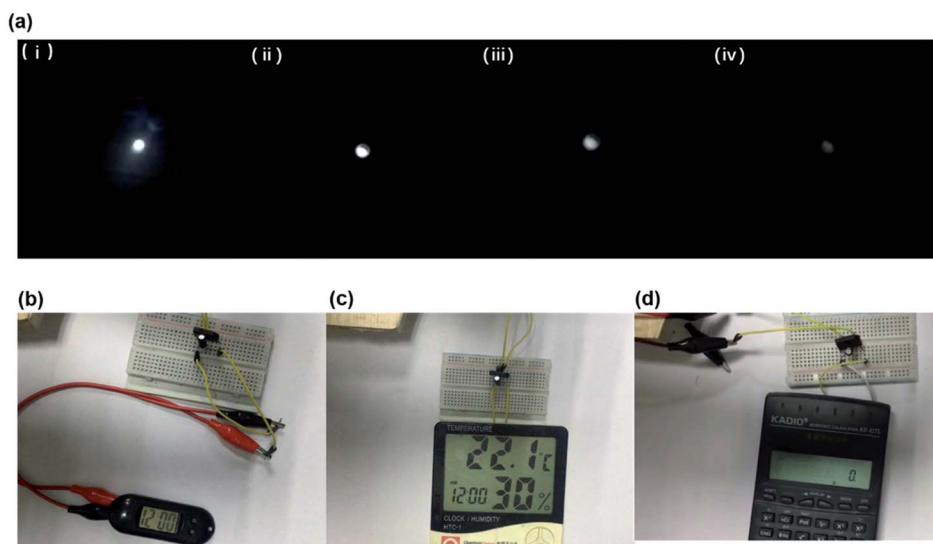
Fig. 4 Application of the 3×3 cm^2 TENG in multiple devices. (a) The TENG was used to illuminate an LED for different time periods: (i) 0 s, (ii) 5 s, (iii) 15 s, and (iv) 30 s. Different electronic devices were driven by the edible TENG, including (b) an electric watch, (c) a temperature–humidity sensor, (d) and a calculator.

capacitors to 3.25 V under 38% RH and 2 Hz operating frequency, which can continuously supply power to the LED, as shown in Fig. 4a and Video S1.† In addition, many different electronic devices could also be powered by the TENG, as shown in Fig. 4b–d. The example devices were electronic watches, temperature and humidity sensors, and calculators. Demo operation (Videos S2–S4) can be found in the ESI.†

3.3. Applications of the edible TENG

Considering that babies like biting things, this non-toxic TENG is rather applicable to baby care products as it will not cause harm after ingestion. As babies often cannot discriminate between food and non-edible items, they may accidentally eat nearby items, such as components of electronic toys. Conventional energy sources for these baby products are supercapacitors[46,47] and lithium batteries.[48] However, small electronic parts can cause serious harm to babies and can even be life threatening, especially button batteries.

Fig. 5b shows the structure and working principle of button batteries. The inside of a button battery is filled with electrolyte.

When a button battery is accidentally eaten, stomach acid will corrode the battery shell and release the electrolyte in the battery. The components of the electrolyte are generally $LiPF_6$, $LiClO_4$, and $LiBF_4$. They corrode gastric mucosa and may cause gastrointestinal bleeding, endangering human life.[23] Therefore, this water-soluble and non-toxic TENG can be used in baby products, such as toys and diaper sensors, so that even if the baby accidentally eats it, it will not cause harm to the baby's health. We designed a diaper based on this kind of TENG, as shown in Fig. 5. The lively baby provides the TENG with sufficient energy to charge the capacitor. When the diaper is wet, the TENG dissolves in the water, and the circuit can be opened by the wet part, and the LED turns on. Demo operation (Video S5) can be found in the ESI.† In this case, the parent will know that the baby has urinated and can change the diaper in time. Meanwhile, the TENG can be used to light up LEDs on babies' toys, which will also avoid the risk introduced by traditional power sources.

Infrared heat dissipation is very helpful for keeping the skin cool under fabric.[49] Children often develop rashes due to poor
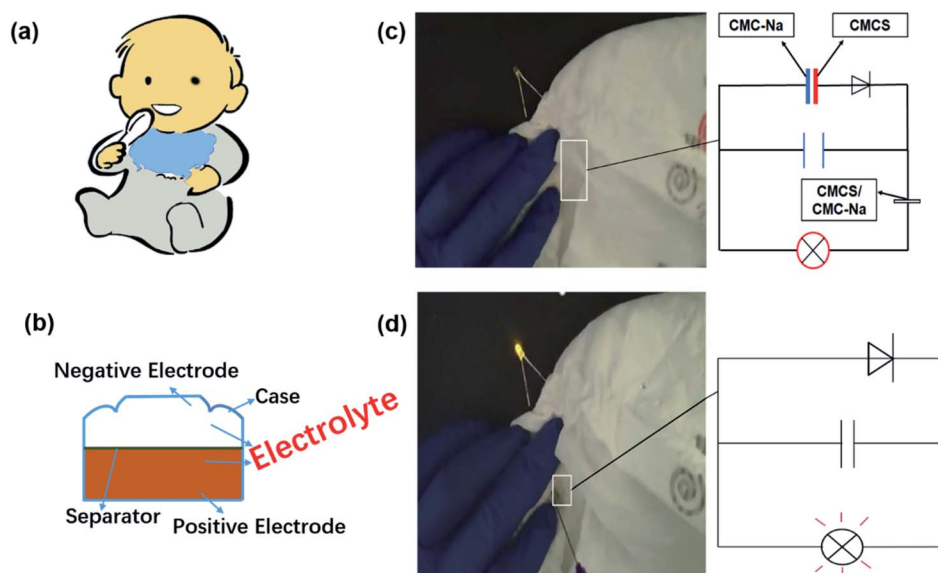
Fig. 5 (a) Babies often eat baby products. (b) Schematic diagram of a button battery, which contains hazardous electrolyte. (c) Physical map and circuit diagram of the edible TENG before operation and (d) after operation.
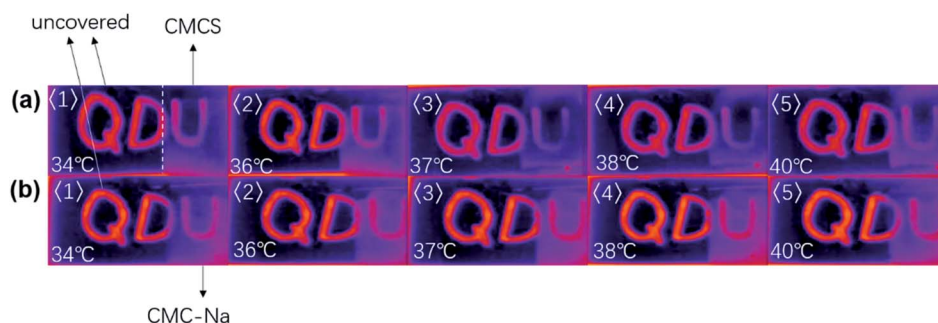
Fig. 6 Thermal radiation performance of (a) CMCS nanofiber membrane and (b) CMC-Na nanofiber membrane at (1) 34 °C, (2) 36 °C, (3) 37 °C, (4) 38 °C, and (5) 40 °C.

heat dissipation in diapers, which can harm their health. This requires the design of diapers with a certain infrared transmission effect. We simulated different temperature environments and tested the permeability of the two nanofiber membranes to thermal radiation. The permeability of thermal radiation can be seen in Fig. 6. In the range of 34 to 40 °C, the membranes have good permeability to thermal radiation, so they will not affect the comfort of the diaper.

Herein, we have demonstrated the applications of the TENG in baby care. Because of the liveliness of children and their vulnerability to toxic substances, the application of edible nanogenerators will reach far beyond the uses we have demonstrated. In the future, more applications can be designed based on edible nanogenerators, and by searching for natural polymer materials with different electronegativities, a series of new, edible, environmentally friendly nanogenerators can be designed.

4. Conclusions

In summary, we reported an edible TENG. It has the characteristics of rapid dissolution in water, non-toxicity and environmental friendliness. The output performance of the TENG with an effective area of 3×3 cm^2 can reach 120 mW m^{-2}. It can continuously power electronic watches, temperature-hygrometers, and calculators. This TENG is applicable in intelligent fabric for babies. The application in a diaper that monitors the urination of babies is demonstrated as an example. At the same time, good heat dissipation performance of the material, taking advantage of its infrared transmittance, can ensure the comfort of diapers. Therefore, this non-toxic TENG is very applicable for baby care. Safer TENGs can be designed based on this idea.

Conflicts of interest

There are no conflicts to declare.

Acknowledgements

References

1 K. Dong, X. Peng and Z.-L. Wang, Fiber/Fabric-Based Piezoelectric and Triboelectric Nanogenerators for Flexible/Stretchable and Wearable Electronics and Artificial Intelligence, *Adv. Mater.*, 2020, **32**, 43.

2 Y. Lee, S.-H. Cha, Y.-W. Kim, D. Choi and J.-Y. Sun, Transparent and attachable ionic communicators based on self-cleanable triboelectric nanogenerators, *Nat. Commun.*, 2018, **9**, 8.

3 Y. Zou, P.-C. Tan, B.-J. Shi, H. Ouyang, D.-J. Jiang, Z. Liu, H. Li, M. Yu, C. Wang, X.-C. Qu, L.-M. Zhao, Y.-B. Fan, Z.-L. Wang and Z. Li, A bionic stretchable nanogenerator for underwater sensing and energy harvesting, *Nat. Commun.*, 2019, **10**, 10.

4 J.-S. Chun, B.-U. Ye, J.-W. Lee, D. Choi, C.-Y. Kang, S.-W. Kim, Z.-L. Wang and J. M. Baik, Boosted output performance of triboelectric nanogenerator via electric double layer effect, *Nat. Commun.*, 2016, **7**, 9.

5 X.-X. Wang, W.-Z. Song, M.-H. You, J. Zhang, M. Yu, Z.-Y. Fan, S. Ramakrishna and Y.-Z. Long, Bionic single-electrode electronic skin unit based on piezoelectric nanogenerator, *ACS Nano*, 2018, **12**, 8588–8596.

6 W.-Z. Song, X.-X. Wang, H.-J. Qiu, Q. Liu, J. Zhang, Z.-Y. Fan, M. Yu, S. Ramakrishna, H. Hu and Y.-Z. Long, Sliding non-contact inductive nanogenerator, *Nano Energy*, 2019, **63**, 103878.

7 R.-Q. Liu, X.-X. Wang, J. Fu, Q.-Q. Zhang, W.-Z. Song, Y. Xu, Y.-Q. Chen, S. Ramakrishna and Y.-Z. Long, Preparation of Nanofibrous PVDF Membrane by Solution Blow Spinning for Mechanical Energy Harvesting, *Nanomaterials*, 2019, **9**, 1090.

8 F.-Q. Chen, Y.-H. Wu, Z.-Y. Ding, X. Xia, S.-H. Li, H.-W. Zheng, C.-L. Diao, G.-T. Yue and Y.-L. Zi, A novel triboelectric nanogenerator based on electrospun polyvinylidene fluoride nanofibers for effective acoustic energy harvesting and self-powered multifunctional sensing, *Nano Energy*, 2019, **56**, 241–251.

9 H.-J. Qiu, W.-Z. Song, X.-X. Wang, J. Zhang, Z.-Y. Fan, M. Yu, S. Ramakrishna and Y.-Z. Long, A calibration-free self-powered sensor for vital sign monitoring and finger tap communication based on wearable triboelectric nanogenerator, *Nano Energy*, 2019, **58**, 536–542.

10 J. Du, L. Wang, Y.-B. Shi, F. Zhang, S.-H. Hu, P.-B. Liu, A.-Q. Li and J. Chen, Optimized CNT-PDMS Flexible Composite for Attachable Health-Care Device, *Sensors*, 2020, **20**, 4523.

11 P. Wang, S. Zhang, L. Zhang, L.-F. Wang, H. Xue and Z.-L. Wang, Non-contact and liquid–liquid interfacing triboelectric nanogenerator for self-powered water/liquid level sensing, *Nano Energy*, 2020, 104703.

12 U. T. Jurado, S.-H. Pu and N. M. White, Grid of hybrid nanogenerators for improving ocean wave impact energy harvesting self-powered applications, *Nano Energy*, 2020, 104701.

13 L.-X. Gao, S. Lu, W.-B. Xie, X. Chen, L.-K. Wu, T.-T. Wang, A.-B. Wang, C.-Q. Yue, D.-Q. Tong and W.-Q. Lei, A Self-Powered and Self-Functional Tracking System Based on Triboelectric-Electromagnetic Hybridized Blue Energy Harvesting Module, *Nano Energy*, 2020, 104684.

14 W.-H. Dong, J.-X. Liu, X.-J. Mou, G.-S. Liu, X.-W. Huang, X. Yan, X. Ning, S. Russell, Y.-Z. Long and C. S. B. Biointerfaces, Performance of polyvinyl pyrrolidone-isatis root antibacterial wound dressings produced in situ by handheld electrospinner, *Colloids Surf., B*, 2020, **188**, 110766.

This journal is © The Royal Society of Chemistry 2020

J. Mater. Chem. A, 2020, **8**, 22745–22753 | **22751**

15 Q. Chang, Y.-F. He, Y.-Q. Liu, W. Zhong, Q. Wang, F. Lu and M. Xing, Protein Gel's Phase Transition: Toward Superiorly Transparent and Hysteresis-Free Wearable Electronics, *Adv. Funct. Mater.*, 2020, **30**, 1910080.

16 F.-Y. Wang, Z.-X. Wang, Y.-X. Zhou, C.-L. Fu and H.-W. Zheng, Windmill-inspired hybridized triboelectric nanogenerators integrated with power management circuit for harvesting wind and acoustic energy, *Nano Energy*, 2020, 105244.

17 F.-R. Fan, Z.-Q. Tian and Z.-L. Wang, Flexible triboelectric generator, *Nano Energy*, 2012, **1**, 328–334.

18 F.-R. Fan, L. Lin, G. Zhu, W.-Z. Wu, R. Zhang and Z.-L. Wang, Transparent Triboelectric Nanogenerators and Self-Powered Pressure Sensors Based on Micropatterned Plastic Films, *Nano Lett.*, 2012, **12**, 3109–3114.

19 G. Zhu, C.-F. Pan, W.-X. Guo, C.-Y. Chen, Y.-S. Zhou, R.-M. Yu and Z.-L. Wang, Triboelectric-generator-driven pulse electrodeposition for micropatterning, *Nano Energy*, 2012, **12**, 4960–4965.

20 Y.-J. Su, G. Zhu, W.-Q. Yang, J. Yang, J. Chen, Q.-S. Jing, Z.-M. Wu, Y.-D. Jiang and Z.-L. Wang, Triboelectric sensor for self-powered tracking of object motion inside tubing, *ACS Nano*, 2014, **8**, 3843–3850.

21 F. Yi, L. Lin, S.-M. Niu, J. Yang, W.-Z. Wu, S.-H. Wang, Q.-L. Liao, Y. Zhang and Z.-L. Wang, Self-powered trajectory, velocity, and acceleration tracking of a moving object/body using a triboelectric sensor, *Adv. Funct. Mater.*, 2014, **24**, 7488–7494.

22 C.-B. Han, C. Zhang, X.-H. Li, L.-M. Zhang, T. Zhou, W.-G. Hu and Z.-L. Wang, Self-powered velocity and trajectory tracking sensor array made of planar triboelectric nanogenerator pixels, *Nano Energy*, 2014, **9**, 325–333.

23 H.-W. Zheng, Y.-L. Zi, X. He, H.-Y. Guo, Y.-C. Lai, J. Wang, S. L. Zhang, C.-S. Wu, G. Cheng and Z.-L. Wang, Concurrent Harvesting of Ambient Energy by Hybrid Nanogenerators for Wearable Self-Powered Systems and Active Remote Sensing, *ACS Appl. Mater. Interfaces*, 2018, **10**, 14708–14715.

24 Y. Yang, G. Zhu, H.-L. Zhang, J. Chen, X.-D. Zhong, Z.-H. Lin, Y.-J. Su, P. Bai, X.-N. Wen and Z.-L. Wang, Triboelectric Nanogenerator for Harvesting Wind Energy and as Self-Powered Wind Vector Sensor System, *ACS Nano*, 2013, **7**, 9461–9468.

25 Y.-S. Zhou, G. Zhu, S.-M. Niu, Y. Liu, P. Bai, Q.-S. Jing and Z.-L. Wang, Nanometer Resolution Self-Powered Static and Dynamic Motion Sensor Based on Micro-Grated Triboelectrification, *Adv. Mater.*, 2014, **26**, 1719–1724.

26 Q.-S. Jing, G. Zhu, W.-Z. Wu, P. Bai, Y.-N. Xie, R. P. S. Han and Z.-L. Wang, Self-powered triboelectric velocity sensor for dual-mode sensing of rectified linear and rotary motions, *Nano Energy*, 2014, **10**, 305–312.

27 Z. H. Lin, G. Zhu, Y.-S. Zhou, Y. Yang, P. Bai, J. Chen and Z.-L. Wang, A self-powered triboelectric nanosensor for mercury ion detection, *Angew. Chem., Int. Ed.*, 2013, **52**, 5065–5069.

28 H.-L. Zhang, Y. Yang, Y.-J. Su, J. Chen, C.-G. Hu, Z.-K. Wu, Y. Liu, C.-P. Wong, Y. Bando and Z.-L. Wang, Triboelectric nanogenerator as self-powered active sensors for detecting liquid/gaseous water/ethanol, *Nano Energy*, 2013, **2**, 693–701.

29 X.-N. Wen, Y.-J. Su, Y. Yang, H.-L. Zhang and Z.-L. Wang, Applicability of triboelectric generator over a wide range of temperature, *Nano Energy*, 2014, **4**, 150–156.

30 D. Han and A. J. Steckl, Triaxial electrospun nanofiber membranes for controlled dual release of functional molecules, *ACS Appl. Mater. Interfaces*, 2013, **5**, 8241–8245.

31 W.-L. Luo, X. Qiu, J. Zhang, P.-Y. Hu, X.-F. Liu, J.-J. Liu, M. Yu, S. Ramakrishna and Y.-Z. Long, In situ accurate deposition of electrospun medical glue fibers on kidney with auxiliary electrode method for fast hemostasis, *Mater. Sci. Eng., C*, 2019, **101**, 380–386.

32 X. Li, X.-X. Wang, T.-T. Yue, Y. Xu, M.-L. Zhao, M. Yu, S. Ramakrishna and Y.-Z. Long, Waterproof-breathable PTFE nano- and Microfiber Membrane as High Efficiency PM2.5 Filter, *Polymers*, 2019, **11**, 590.

33 W. Liang, Y. Xu, X. Li, X.-X. Wang, H.-D. Zhang, M. Yu, S. Ramakrishna and Y. Z. Long, Transparent Polyurethane Nanofiber Air Filter for High-Efficiency PM2.5 Capture, *Nanoscale Res. Lett.*, 2019, **14**, 361.

34 X.-X. Wang, N. Wang, H.-J. Qiu, W.-Z. Song, Q. Liu, Z.-Y. Fan, M. Yu, S. Ramakrishna and Y.-Z. Long, Anisotropic nanogenerator for anticounterfeiting and information encrypted transmission, *Nano Energy*, 2020, **71**, 104572.

35 L. Wang, J.-C. Yang, B. Ran, X.-L. Yang, W.-F. Zheng, Y.-Z. Long and X.-Y. Jiang, Small Molecular TGF-beta 1-Inhibitor-Loaded Electrospun Fibrous Scaffolds for Preventing Hypertrophic Scars, *ACS Appl. Mater. Interfaces*, 2017, **9**, 32545–32553.

36 Q.-Q. Zhang, X.-X. Wang, J. Fu, R.-Q. Liu, H.-W. He, J.-W. Ma, M. Yu, S. Ramakrishna and Y. Z. Long, Electrospinning of Ultrafine Conducting Polymer Composite Nanofibers with Diameter Less than 70 nm as High Sensitive Gas Sensor, *Materials*, 2018, **11**, 10.

37 D.-Y. Zhu, Y. Xu, X.-X. Wang, J.-X. Sui, Q. Liu, C. Song, J. Yu, J.-P. Wu and Y.-Z. Long, Preparation of indium oxide by electrospinning and its electromagnetic properties at low temperature, *J. Magn. Magn. Mater.*, 2020, **501**, 5.

38 Q. Liu, S. Ramakrishna and Y.-Z. Long, Electrospun flexible sensor, *J. Semicond.*, 2019, **40**, 1674–4926.

39 T.-T. Yue, X. Li, X.-X. Wang, X. Yan, M. Yu, J.-W. Ma, Y. Zhou, S. Ramakrishna and Y. Z. Long, Electrospinning of Carboxymethyl Chitosan/Polyoxyethylene Oxide Nanofibers for Fruit Fresh-Keeping, *Nanoscale Res. Lett.*, 2018, **13**, 239.

40 S. K. Sahu, S. K. Mallick, S. Santra, T. K. Maiti, S. K. Ghosh and P. Pramanik, In vitro evaluation of folic acid modified carboxymethyl chitosan nanoparticles loaded with doxorubicin for targeted delivery, *J. Mater. Sci.: Mater. Med.*, 2010, **21**, 1587–1597.

41 R. Krishna and J. K. Pandit, Carboxymethylcellulose-sodium based transdermal drug delivery system for propranolol, *J. Pharm. Pharmacol.*, 1996, **48**, 367–370.

42 X.-X. Wu, M.-J. Yun, M. Wang, C. Liu, K. Li, X.-H. Qin, W.-J. Kong and L.-F. Dong, Self-imaging in multi-walled carbon nanotube arrays at visible wavelengths, *Carbon*, 2016, **108**, 47–51.

22752 | *J. Mater. Chem. A*, 2020, **8**, 22745–22753

This journal is © The Royal Society of Chemistry 2020

43 G. Khandelwal, T. Minocha, S. K. Yadav, A. Chandrasekhar, N. P. M. J. Raj, S. C. Gupta and S.-J. Kim, All edible materials derived biocompatible and biodegradable triboelectric nanogenerator, *Nano Energy*, 2019, **65**, 104016.

44 M.-H. You, X.-X. Wang, X. Yan, J. Zhang, W.-Z. Song, M. Yu, Z.-Y. Fan, S. Ramakrishna and Y.-Z. Long, A self-powered flexible hybrid piezoelectric–pyroelectric nanogenerator based on non-woven nanofiber membranes, *J. Mater. Chem. A*, 2018, **6**, 3500–3509.

45 Z.-L. Li, J.-L. Shen, I. Abdalla, J.-Y. Yu and B. Ding, Nanofibrous membrane constructed wearable triboelectric nanogenerator for high performance biomechanical energy harvesting, *Nano Energy*, 2017, **36**, 341–348.

46 G.-T. Xia, C. Li, K. Wang and L.-W. Li, Structural design and electrochemical performance of PANI/CNTs and MnO2/CNTs supercapacitor, *Sci. Adv. Mater.*, 2019, **11**, 1079–1086.

47 Y.-T. Zhou, Y.-N. Huang, J.-B. Pang and K. Wang, Remaining useful life prediction for supercapacitor based on long short-term memory neural network, *J. Power Sources*, 2019, **440**, 227149.

48 S.-T. Fan, J. Zhang, X.-L. Teng, X. Wang, H.-S. Li, Q. Li, J. Xu, D.-R. Cao, S.-D. Li and H. Hu, Self-Supported Amorphous SnO2/TiO2 Nanocomposite Films with Improved Electrochemical Performance for Lithium-Ion Batteries, *J. Electrochem. Soc.*, 2019, **166**, A3072–A3078.

49 N.-N. Shi, C.-C. Tsai, F. Camino, G.-D. Bernard, N. Yu and R. Wehner, Keeping cool: enhanced optical reflection and radiative heat dissipation in Saharan silver ants, *Science*, 2015, **349**, 298–301.

This journal is © The Royal Society of Chemistry 2020

J. Mater. Chem. A, 2020, **8**, 22745–22753 | **22753**